https://doi.org/10.5607/en22028
Exp Neurobiol. 2022 Dec;31(6):361-375.
pISSN 1226-2560 • eISSN 2093-8144

Original Article

Experimental Neurobiology

Dopamine Receptor Supports the Potentiation of Intrinsic Excitability and Synaptic LTD in Temporoammonic-CA1 Synapse

Hye-Hyun Kim[1,2‡], Suk-Ho Lee[1,2], Won-Kyung Ho[1,2*] and Kisang Eom[3*]
[1]Department of Physiology, Seoul National University College of Medicine, Seoul 03080,
[2]Neuroscience Research Center, Seoul National University College of Medicine, Seoul 03080,
[3]Department of Physiology, School of Medicine, Keimyung University, Daegu 42601, Korea

Dopaminergic projection to the hippocampus from the ventral tegmental area or locus ceruleus has been considered to play an essential role in the acquisition of novel information. Hence, the dopaminergic modulation of synaptic plasticity in the hippocampus has been widely studied. We examined how the D1 and D2 receptors influenced the mGluR5-mediated synaptic plasticity of the temporoammonic-CA1 synapses and showed that the dopaminergic modulation of the temporoammonic-CA1 synapses was expressed in various ways. Our findings suggest that the dopaminergic system in the hippocampal CA1 region regulates the long-term synaptic plasticity and processing of the novel information.

Key words: Dopamine, Temporoammonic pathway, CA1, LTD

INTRODUCTION

Hippocampus plays an important role for the formation of spatial or episodic memories [1, 2]. In addition, the hippocampus is known to perform the function of recognizing new information by comparing existing memories with new information [3]. Previous studies suggest that processing of novel information would be involved in hippocampal CA1 region, especially synapses that relay from direct temporoammonic (TA) input from the entorhinal cortex (EC) to the pyramidal cells of CA1 region (herafter 'TA-CA1 synapse') [4]. It is known that various neuromodulator receptors are distributed in the CA1 region, including dopamine receptors [5]. Previous studies have shown that the dopaminergic modulation of the TA inputs to CA1 region play a role in the detection of spatial novelty and memory retention [4]. These previous studies suggested that the dopaminergic modulation of the TA-CA1 synapses would be important to various hippocampal functions.

Dopaminergic receptors are classified into two groups: D1-like receptors (including the D1 and D5 receptors) and D2-like receptors (including the D2, D3, and D4 receptors), which are relayed to G-proteins [6-8]. The role of each type of dopamine receptor has been mainly studied in the basal ganglia, and revealed that each type of receptor is involved in the different functions of neural circuits [9]. Studies of the dopaminergic receptors, particularly the D1 and D2 receptors, have revealed that the synaptic/intrinsic function in various regions, including the prefrontal cortex (PFC), is regulated by dopaminergic receptors; they have also revealed the relationships between dopaminergic modulation and animal behavior [10-12]. For dopaminergic modulation in the PFC neurons, the interaction between the metabolic glutamate receptor type 5 (mGluR5) and dopamine receptors have been widely studied

Submitted August 11, 2022, Revised November 15, 2022,
Accepted December 28, 2022

*To whom correspondence should be addressed.
Kisang Eom, TEL: 82-53-258-7416, FAX: 82-53-258-7412
e-mail: hitiet21@gmail.com
Won-Kyung Ho, TEL: 82-2-740-8226, FAX: 82-2-763-9667
e-mail: wonkyung@snu.ac.kr
‡Hye-Hyun Kim's Present address: Department of Physiology, Michigan State University, East Lansing, MI 48824, USA

[13-15]. However, studies for each dopamine receptor and their signaling pathways involved with synaptic modulation in the hippocampus have been relatively insufficient.

Previously, we showed that the potentiation of intrinsic excitability (PIE) of the pyramidal cells of the CA1 (CA1-PC) was accompanied by long-term depression (LTD) induced by low-frequency stimulation (LFS) at the Schaffer collateral (SC)-CA1 synapses [16]. Although the dopaminergic modulation of the SC-CA1 synapses that receive inputs from the CA3 pyramidal cells has been widely studied [17], studies of the TA-CA1 synapse and its dopaminergic modulation have been relatively insufficient. Here, we studied LTD in the TA-CA1 synapses and its accompanying EPSP-to-Spike potentiation (E-S potentiation is an activity-dependent form of plasticity that boosts the efficiency of the coupling between the synaptic input and the action potential output in a neuron) in the CA1-PCs and their mechanisms. We discovered a novel form of long-term potentiation (LTP)/LTD modulation in the TA-CA1 synapses, which is caused by dopamine. Our results provide clues as to how dopamine contributes to the formation and operation of the neural representation in the hippocampus.

MATERIALS AND METHODS

Animals

All experiments were conducted with the approval of the animal experiment ethics committee at the Seoul National University College of Medicine (MD-11-A251). Experiments were conducted in Sprague-Dawley rats at postnatal days 15~24, and the total number of animals used was described in below. The animals were maintained in standard environmental conditions (temperature: 25±2℃, humidity: 60±5%, dark/light cycle: 8:00 p.m.~8:00 a.m. of next day/8:00 a.m.~8:00 p.m.) and monitored under veterinary supervision.

Slice preparation

Acute transverse slices of intermediate/ventral hippocampus were obtained from juvenile rats (postnatal days 15~24) of either sex, unless specified otherwise. Rats were anesthetized by inhalation of 5% isoflurane. After decapitation, brains were immediately removed and submerged in an ice-cold preparation solution containing the following (in mM): NaCl 116, $NaHCO_3$ 26, KCl 3.2, NaH_2PO_4 1.25, $CaCl_2$ 0.5, $MgCl_2$ 7, glucose 10, Na-pyruvate 2, and vitamin C 3. The acute transverse slices (300 μm thick) were prepared using a vibratome (VT1200S, Leica Microsystems). Slices were maintained at room temperature, and then data were acquired at 32℃ in a recording solution containing the following (in mM): NaCl 124, $NaHCO_3$ 26, KCl 3.2, NaH_2PO_4 1.25, $CaCl_2$ 2.5, $MgCl_2$ 1.3, and glucose 10. The preparation solution and recording solution were continuously aerated with mixture of 95% O_2 and 5% CO_2 to a final pH of 7.4. Detailed procedures for slice preparation is annotated in the previous study [16].

Electrophysiology recordings

Hippocampal slices were transferred to an immersed recording chamber continuously perfused with oxygenated recording solution using a peristaltic pump (Gilson Miniplus 3; Gilson, Middleton, WI, USA). CA1-PCs were visualized using an upright microscope equipped with differential interference contrast optics (BX51WI, Olympus, Shizuoka, Japan). All electrophysiological recordings were made in soma with an EPC-8 amplifier (HEKA Electronik, Lambrecht, Germany) at a sampling rate of 10 kHz. All the recordings were performed at 32±1℃, and perfusion rate of the recording solution was maintained at 1~1.5 ml/min. Patch pipettes (3~4 MΩ) and monopolar glass electrode (1~2 MΩ) were made from glass capillaries (Borosilicate glass capillaries) using a puller (PC-10, Narishige, Tokyo, Japan). The pipettes were filled with internal solutions containing the following (in mM): potassium gluconate 130, KCl 7, $NaCl_2$, $MgCl_2$ 1, EGTA 0.1, ATP-Mg 2, Na-GTP 0.3, and HEPES 10 (pH=7.3 with KOH, 295 mOsm with sucrose). Somatic (positive or negative) current injections were done at the holding potential -65 mV unless otherwise indicated.

Synaptic stimulation

Based on previous study [16], A stimulator (Stimulus Isolator A360; WPI, Sarasota, FL, USA) connected to the monopolar glass electrode filled with the recording solution was placed in the stratum lacunosum-moleculare (SLM; horizontally 150 μm and vertically 300~350 μm away from the top layer of soma) or stratum radiatum (SR; horizontally and vertically 120~150 μm away from the top layer of soma) of the CA1 region to evoke excitatory postsynaptic current (EPSC) of TA-CA1 or SC-CA1 synapses, respectively. For the EPSC of TA-CA1 synapses (hereafter TA-EPSC) or SC-CA1 synapses (hereafter SC-EPSC), the stimulus intensity (duration: 0.1 ms; stimulus intensity: 9~31.5 V) of extracellular stimulation was adjusted to evoke current amplitudes between 100 pA and 300 pA for the baseline. During the whole-cell configuration, pipette series resistance and membrane capacitance were compensated manually and checked throughout the experiment [18]. Cells in which the series resistance exceeded 20 MΩ and changed 15% during the experiment were discarded. The TA-EPSCs or SC-EPSCs were recorded from CA1-PCs with whole-cell configuration at a holding potential of -63 mV, which were evoked by paired pulses with 50 msec which were delivered every 10 secs through stimulation electrodes placed in SLM (TA-EPSC) or SR (SC-EPSC)

https://doi.org/10.5607/en22028

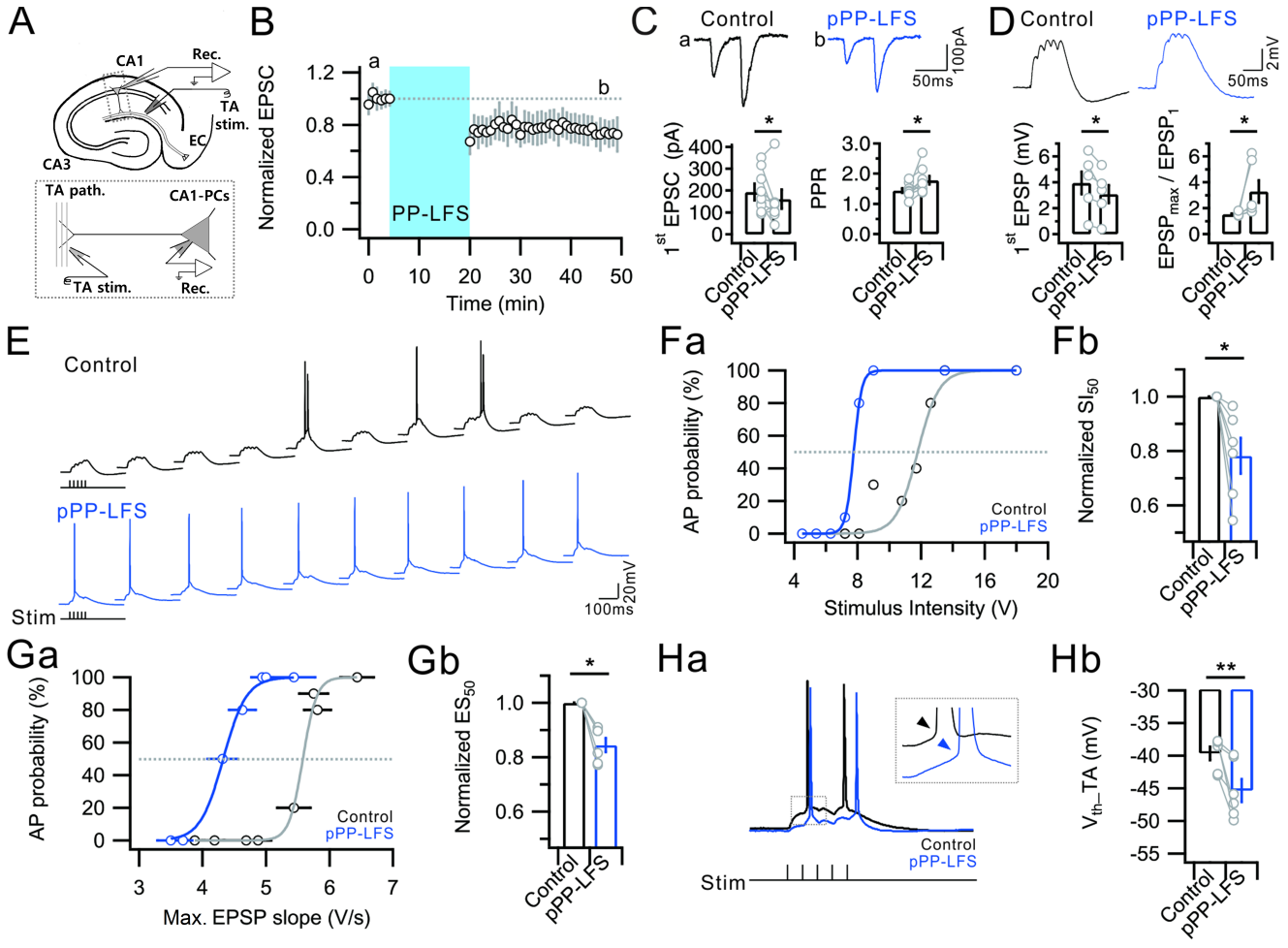

Fig. 1. Induction of E-S potentiation during the LTD by PP-LFS of SLM. (A) *Upper*: Recording set up. A whole-cell configuration was established in CA1-PCs of hippocampal slice. Stimulating electrodes were placed in the CA1-SLM. The gray box that contains CA1-PCs and axons from entorhinal cortex was magnified to lower figure. *Lower*: Magnified image from gray box in the upper figure. Glass monopolar electrode was placed near the distal dendrites of CA1-PCs and whole-cell configuration was formed in CA1-PC soma. (B) The PP-LFS of TA-CA1 synapses induced TA-LTD amplitude. (C) *Upper*: Representative TA-EPSCs recorded before PP-LFS induction (a, Control) and 25~30 min after PP-LFS (b, pPP-LFS). *Lower, left*: Change of 1st TA-EPSC for the control and pPP-LFS. *Lower, right*: Change of PPR for the control and pPP-LFS. (D) *Upper*: Voltage responses to 5 pulses at 50 Hz of subthreshold stimulation for the control and the pPP-LFS. *Lower, left*: 1st EPSP amplitude for the control and pPP-LFS. *Lower, right*: Ratio between the amplitude of maximal depolarization ($EPSP_{max}$) evoked by the 5 pulses at 50 Hz and 1st EPSP amplitude ($EPSP_{max}/EPSP_1$ ratio) for the control and the pPP-LFS. (E) Raw voltage traces as a result of 10 trials of TA burst stimulation (5 stimuli, 50 Hz, 2 s interval) for the control and the pPP-LFS. For the pPP-LFS, the 10 trials of TA bursts triggered firing in all trials, in contrast of the control. (Fa) Graph showing distribution of AP probability as a function of stimulus voltage for the control and pPP-LFS. (Fb) Bar graphs and circles represent that average and individual normalized SI_{50} is significantly decreased after PP-LFS, respectively. (Ga) Graph showing distribution of firing probability as a function of Max. EPSP slope for the control and the pPP-LFS. (Gb) Bar graphs and circles represent that average and individual Normalized ES_{50} is significantly decreased after PP-LFS, respectively. (Ha) Voltage responses to 5 trials of suprathreshold TA burst stimulation for the control and the pPP-LFS. *Insets*: Change of V_{th}_TA for the control and the pPP-LFS were indicated with arrowheads. (Hb) Bar graphs representing significant V_{th} hyperpolarization that AP induced by theTA burst stimulation (V_{th}_TA). Error bars indicate SEM. For the experiments of Figure 1, 9 mice were used.

of CA1 region (hereafter 'test pulses'). Schematic diagram of electrode positions was illustrated as Fig. 1A. After the establishment of the baseline EPSC (see Results), LTD was induced by applying low-frequency stimulation consists of paired pulses (PP-LFS) which is comprised of 900 paired pulses (50 msec interval) delivered every 1 sec to TA or SC pathway in current-clamp mode with the same stimulus intensity used for baseline EPSC recordings [19]. After the induction of LTD, the test pulses with same intensity as the baseline EPSCs were delivered the glass electrodes until the end of recording. All recordings were performed in the presence of an NMDAR antagonist (AP-5 50 μM) to block NMDAR dependent effects. For evaluation of E-S potentiation in TA-CA1

synapses, 10 TA bursts which consisted of 5 pulses at 50 Hz (Fig. 1E) were delivered every 10 sec before (control; delivered at time 'a' in Fig. 1B) and after the PP-LFS (post PP-HFS [hereafter 'pPP-LFS']; delivered at time 'b' in Fig. 1B). The number of bursts that evoked APs and their V_{th} were measured in the control and the pPP-LFS. Paired pulse ratio (PPR) of the test pulses was calculated as ratio between the amplitude of 2nd EPSC and 1st EPSCs those measured from the baseline evoked by test pulses.

Potassium current recordings

Somatic K^+ outward current was recorded in the voltage-clamp mode in the presence of synaptic blockers (plus an inward current blocker cocktail that consisted of 500 μM Ni^{2+}, 300 μM Cd^{2+} and 0.5 μM tetrodotoxin (TTX) in order to block voltage-dependent Ca^{2+} and fast Na+ channels. The pulse protocol for measuring membrane K^+ currents was comprised 500 msec depolarization steps from -30 mV to +50 mV, with 10 mV increment from a holding potential of -70 mV. The sustained current (I_{SS}) amplitude was measured as the value of somatic K^+ outward current at the end of the depolarization pulse. After the establishment of whole cell configuration of CA1-PCs, the depolarization steps were applied to measure baseline K^+ currents. Because blocking of Na^+ and Ca^{2+} current was required to measure K^+ current, it is not possible to measure both K^+ current before and after PP-LFS in a single CA1-PC. Therefore, the baseline K^+ current and the K^+ current after PP-LFS were measured in different cells, respectively.

Data analysis

Resting membrane potential (RMP) of CA1-PCs was measured as the membrane potential when no current was injected through the recording electrode after 5 min of whole-cell configuration. An ascending triangular ramp current (250 pA/s) for 1 sec was delivered to CA1-PCs during whole-cell configuration to measure AP threshold (V_{th}) and the number of APs of CA1-PCs (AP #). To measure membrane resistance (R_{in}) and voltage sag, hyperpolarizing current pulses which was comprised 500 msec hyperpolarizing steps from -250 pA to 0 pA, with 25 pA increment from holding current which adjusts membrane potential of CA1-PCs to -65 mV (Supplemental Fig. 2, 3). The R_{in} of CA1-PC was calculated from the voltage deflection induced by the injection of -25 pA hyperpolarized current, according to a previous study [20]. Voltage sag in response to the hyperpolarization current was compared with the voltage sag ($V_{sag}=V_{max}-V_{ss}$) versus V_{max} (Supplemental Fig. 2). In the case of R_{in} and V_{sag} of CA1-PC, the results measured at -65 mV and those measured at RMP were the same, so the above two values were measured and calculated at RMP. The V_{th} evoked by ramp current injection (V_{th}_ramp) or synaptic stimulation (V_{th}_TA) was determined by the potential where dV/dt of voltage trace exceeds 10 V/s. We confirmed that V_{th} was not significantly affected by the TA stimulation intensity. We obtained V_{th} from at least five APs, and the averaged value was regarded as the V_{th} of the cell in each experimental condition. Recordings to compare V_{th} were done at a sampling rate of 10~50 kHz. The AP probability was measured by the success or failure of AP generation during the trials [(n/10)×100(%)] (See results). From synaptic-stimuli trials with various stimulus intensity, the Max. EPSP slope was measured from the derivative of the first EPSP within 2 msec from the stimulation time. Plotted AP probability along stimulus intensity or the Max. EPSP slope was fitted with sigmoid function.

Drugs

AP-V, bicuculline, CNQX, CGP52432, MPEP, SCH23390, Sulpiride, picrotoxin and tetrodotoxin were purchased from Tocris Bioscience (Bristol, UK). Stock solutions of these drugs were made by dissolution in deionized water or DMSO and were stored at 20℃. During the experiment, one aliquot was thawed and used. The DMSO concentration in solutions was maintained 0.1%.

Statistical analysis

The data were analyzed using IgorPro (version 4.1, WaveMetrics) and OriginPro (version 8.0, Microcal, MA, USA) software and presented as mean±SEM (standard error of mean). Statistical data were evaluated for normality and variance equality with Kolmogorov–Smirnov (K–S) test and Levene's test, respectively. If data were not satisfied with normality or variance equality, nonparametric tests such as Wilcoxon signed-rank test were used. In the Fig. 1 and 2, Student's paired *t*-test, Wilcoxon signed-rank test was used to evaluate statistical significance. Statistical parameters (*t*-value or Z-value) and significance level (as p-value) were reported in the Results section. In the Fig. 3, RM-ANOVA and 2-way ANOVA was used to evaluate statistical significance, and *F*-value and p-value was reported. In the Fig. 4, paired *t*-test was used to evaluate statistical significance, and *t*-value and p-value were reported. Bonferroni posthoc test and simple main effect analysis were used to in-depth analysis. The number of samples (i.e. neurons) and statistical tests for determining statistical significance were stated in the text and figures using following abbreviations: n.s.: no statistical significance; *: p<.05; **: p<.01; ***: p<.005.

RESULTS

The PP-LFS of the SLM in the CA1-induced E-S potentiation in association with LTD

In a previous study, we found that the mGluR5-dependent LTD

https://doi.org/10.5607/en22028

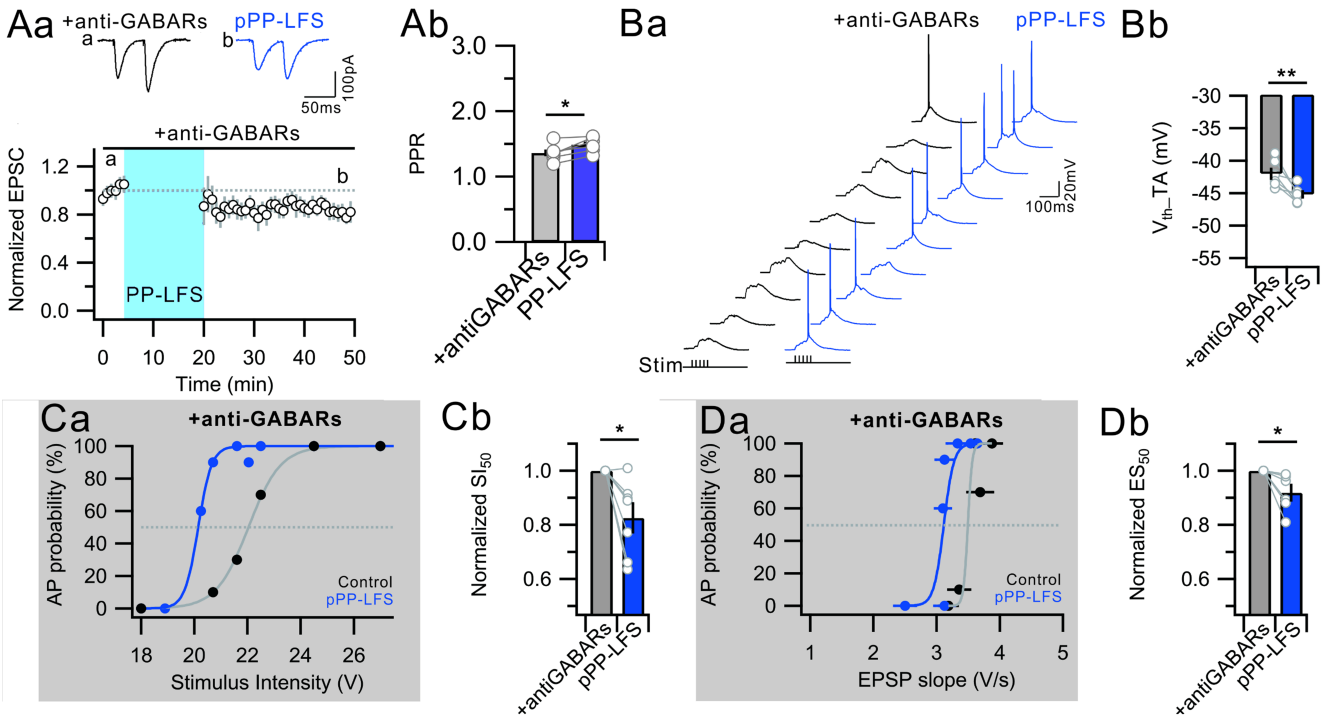

Fig. 2. The $GABA_R$ blockers did not occlude the E-S potentiation associated with V_{th} hyperpolarization during the TA-LTD. (Aa) Application of the anti-GABARs did not abolish TA-LTD after the PP-LFS. *Insets*: The representative EPSCs recorded before the PP-LFS induction (a, Control) and 25~30 min after the PP-LFS (b, pPP-LFS). (Ab) Change of PPR for the control and pPP-LFS under the presence of anti-GABARs. (Ba) Raw voltage traces as a result of 10 trials of TA burst stimulation (5 stimuli, 50 Hz, 2 s interval) for the control and the pPP-LFS. (Bb) Bar graphs representing significant V_{th} hyperpolarization that the AP induced by TA suprathreshold burst stimulation (V_{th}_TA). (Ca) Graph showing distribution of the AP probability as a function of stimulus voltage before for the control and the pPP-LFS. AP probability was obtained from 10 trials at each stimulus intensity. (Cb) Bar graphs and circles represent the average and individual normalized SI_{50}, respectively, which is significantly decreased after the PP-LFS. (Da) Graph showing the distribution of the firing probability as a function of the Max. EPSP slope (Control) and 30 min after the PP-LFS (pPP-LFS). The firing probability was obtained from 10 trials at each stimulus intensity. (Db) Bar graphs and circles represent the average and individual normalized ES_{50}, respectively. Error bars indicate the SEM. For the experiments of Figure 2, 7 mice were used.

at the SC-CA1 synapses was accompanied by the LTD of the inhibitory synapses and the E-S potentiation of the CA1-PCs [16]. It is well known that the CA1-PCs receive excitatory inputs that originate from the EC through the TA pathway to synapses at the distal dendrites of the CA1-PCs [21]. We posed the question of whether the TA-CA1 synapses also expressed LTD and E-S potentiation and whether different mechanisms were involved. A monopolar glass electrode was placed in the SLM of the CA1 area to evoke TA-EPSCs at a holding potential of -63 mV (Fig. 1A). The baseline EPSCs were recorded through paired pulses at a 50-msec interval delivered every 10 s for 5 min, prior to the PP-LFS being applied for 15 min in the current clamp configuration (Fig. 1A, 1B; see Materials and Methods). The detailed LTD induction protocol is described in the Materials and Methods section. TA-EPSC amplitude was evoked after the PP-LFS (193.78±38.71 to 160.78±44.54 pA, 9 neurons, t=-2.965, p=0.018, paired t-test; Fig. 1B, 1C). This depression of the TA-EPSCs lasted more than 30 min, indicating that the PP-LFS of the SLM induced the LTD of the TA-EPSCs (hereafter 'TA-LTD'). The amplitude of the first TA-EPSCs and the PPR of the TA-EPSCs evoked by the TA-paired pulses increased after the PP-LFS (1.41±0.02 to 1.78±0.13, 9 neurons, t=-2.639, p=0.03, paired t-test; Fig. 1C). The presence of the application of the metabolic glutamate receptor 5 antagonist (mGluR5 antagonist, 25 μM MPEP) abolished the TA-LTD induction (106.34±12.15 to 103.88±12.85 pA, 5 neurons from 5 animals, t=0.574, p=0.596, paired t-test; Supplemental Fig. 1) and induced a change in the PPR (1.41±0.02 to 1.51±0.06, 5 neurons from 5 animals, t=0.162, p=0.879, paired t-test; Supplemental Fig. 1). These results suggest that activation of the mGluR5 are essential for the induction of the TA-LTD. By the PP-LFS, the excitatory postsynaptic potential (EPSP) induced by a TA burst stimulation (five pulses at 50 Hz), which was delivered by the monopolar glass pipette in the CA1-SLM, showed a decrease in the 1st EPSP ($EPSP_1$; Control, 3.96±1.01 mV; pPP-LFS: 3.08±0.82 mV; 5 neurons; t=2.922,

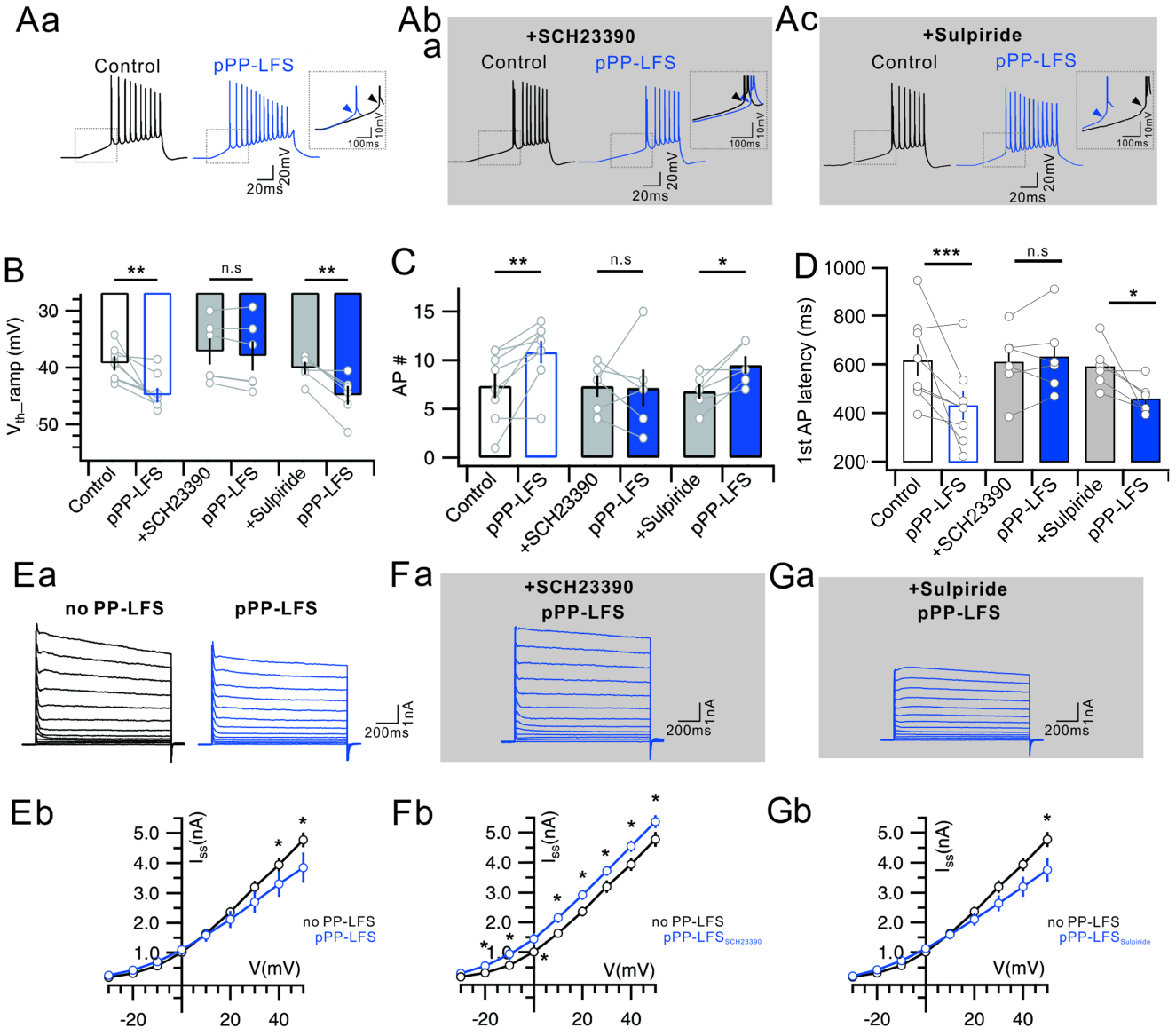

Fig. 3. D1-dependent decrease in the K^+ current underlies the PP-LFS induced the E-S potentiation. (Aa) Representative voltage responses to a ramp (250 pA/s) current injection to soma before (Control) and 30 min after PP-LFS (pPP-LFS). *Inset*: Superimposed traces of significant V_{th} hyperpolarization and shortened latency of the 1st AP. (Ab) Representative voltage responses to a ramp (250 pA/1 s) current injection to soma for the control and the pPP-LFS during the bath application of SCH23390. *Inset*: Superimposed traces of significant V_{th} hyperpolarization and shortened latency of the 1st AP. (Ac) Representative voltage responses to a ramp (250 pA/1 s) current injection to soma for the control and pPP-LFS during the bath application of sulpiride. *Insets*: Superimposed traces of significant V_{th} hyperpolarization and shortened latency of the 1st AP. (B) Bar graphs of V_{th} hyperpolarization (V_{th}_ramp) before (no PP-LFS; *left*: control, *middle*: SCH23390, *right*: sulpiride) and after the PP-LFS (+pPP-LFS) (Time: $F_{(1,17)}$=28.987, p<0.001, Cond: $F_{(2,17)}$=3.181, p=0.067, Time×Cond: $F_{(2,17)}$=4.299, p=0.03; RM-ANOVA and simple effect analysis). (C) Bar graphs of number of AP (AP #) before (no PP-LFS; *left*: control, *middle*: SCH23390, *right*: sulpiride) and after the PP-LFS (+pPP-LFS) (Time: $F_{(1,17)}$=8.550, p=0.009, Cond: $F_{(2,17)}$=2.633, p=0.101, Time×Cond: $F_{(2,17)}$=2.633, p=0.101; RM-ANOVA and simple effect analysis). (D) Bar graphs of 1st AP latency before (no PP-LFS; *left*: control, *middle*: SCH23390, *right*: sulpiride) and after the PP-LFS (+pPP-LFS) (Time: $F_{(1,17)}$=28.987, p<0.00, Cond: $F_{(2,17)}$=3.181, p=0.067, Time×Cond: $F_{(2,17)}$=4.299, p=0.03; RM-ANOVA and simple effect analysis). 20 neurons were used to measuring parameters of intrinsic excitability in Figure 3A~3D. (Ea) Voltage deflections in response to a series of current steps (-30 mV to +50 mV, 10 mV increment) before (no PP-LFS; 7 neurons, left) and after the PP-LFS (pPP-LFS; 5 neurons, right). (Eb) There is slight decrease of K^+ currents during the TA-LTD evoked by the PP-LFS. (Fa) Voltage deflections in response to a series of current steps (-30 mV to +50 mV, 10 mV increment) before (no PP-LFS, left) and after the PP-LFS (pPP-LFS, right). (Fb) Application of D1 blocker (SCH23390; 6 neurons) did not decreased K^+ current after the PP-LFS, but increased the current after the PP-LFS. (Ga) Voltage deflections in response to a series of current steps (-30 mV to +50 mV, 10 mV increment) before (no PP-LFS, left) and after the PP-LFS (pPP-LFS, right) during the bath application of sulpiride (6 neurons). (Gb) Application of D2 blocker, sulpiride, decreased K^+ current after the PP-LFS. (Figure 3E~3G: Cond: $F_{(3,220)}$=0.00, p=1.00; voltage: $F_{(9,220)}$<0.001, p=1.00; voltage×Cond: $F_{(27,220)}$<0.001, p=1.00; 2-way ANOVA and simple main effect analysis; Figure 3E~3G). For the experiments of Figure 3, 44 mice were used.

https://doi.org/10.5607/en22028

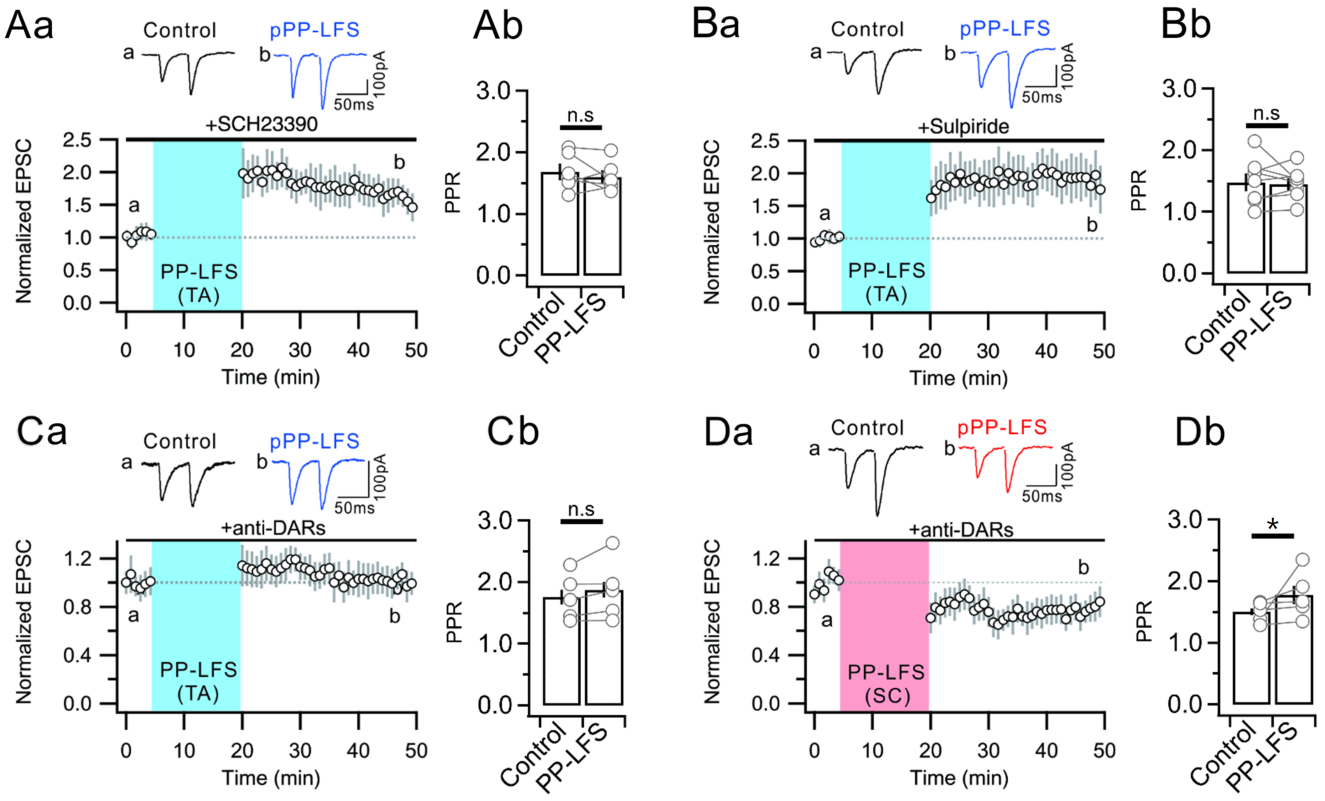

Fig. 4. Contribution of the dopamine receptors to the TA-LTD. (Aa) The PP-LFS to the TA-CA1 synapses induced the LTP of the TA-EPSC amplitude under the SCH23390. Top, representative EPSCs recorded before the induction of the PP-LFS (a, Control) and 25~30 min after the PP-LFS (b, pPP-LFS). (Ab) The PP-LFS to the TA-CA1 synapses did not change the PPR of the TA-CA1 synapses under the SCH23390. (Ba) The PP-LFS of the SLM induced the LTP of the TA-EPSC amplitude under the sulpiride. Top, representative EPSCs recorded before the induction of the PP-LFS (a, Control) and 25~30 min after the PP-LFS (b, pPP-LFS). (Bb) The PP-LFS to the TA-CA1 synapses did not change the PPR of the TA-CA1 synapses under the sulpiride. (Ca) The PP-LFS of the SLM under the anti-DARs (co-application of SCH23390 and sulpiride) transiently increased the TA-EPSC; however, the increase was not sustained. Top, representative EPSCs recorded before the induction of the PP-LFS (a, Control) and 25~30 min after the PP-LFS (b, pPP-LFS). (Bb) The PP-LFS to the TA-CA1 synapses did not change the PPR of the TA-CA1 synapses under the anti-DARs. (Da) The SC-LFS at the Schaffer collateral (SC) under the anti-DARs (co-application of SCH23390 and sulpiride) induced the LTD of the TA-EPSC. Top, representative EPSCs recorded before the induction of the PP-LFS (a, Control) and 25~30 min after the PP-LFS (b, pPP-LFS). (Db) The PP-LFS to the TA-CA1 synapses did not change the PPR of the SC-CA1 synapses under the anti-DARs.

p=0.043; paired *t*-test), but the maximal depolarization evoked by the TA burst stimulation ($EPSP_{max}$) increased, resulting in an increased EPSP summation ratio (Control: 1.53±0.06, six neurons; pPP-LFS: 3.29±0.86; six neurons; Z=-2.201, p=0.028; Wilcoxon signed rank test; Fig. 1D). The increased temporal EPSP summation after the PP-LFS was accompanied by the TA-LTD, as shown in Fig. 1B~1D. The potentiation of the EPSP summation, shown in Fig. 1D, could be associated with E-S potentiation, an activity-dependent plasticity that boosts the efficacy of coupling between the synaptic input and the AP output.

To evaluate the E-S reinforcement of the TA-CA1 synapses, we delivered TA burst stimuli consists of 10 TA bursts which consisted of 5 pulses at 50 Hz through glass monopolar electrodes placed on the SLM of the CA1 region. The stimulus intensity was adjusted from a subthreshold to suprathreshold level to elicit various numbers of APs from the CA1-PCs (Fig. 1E). The PP-LFS evoked the E-S potentiation of the TA-CA1 synapses, which was represented by an increased number of APs after the PP-LFS (Fig. 1Fa). The AP probability was increased after the PP-LFS, compared to the control (Fig. 1Fa, 1Fb). The definition of AP probability was described in Materials and Methods section. The relationship between the AP probability and stimulus intensity was plotted as graph and fitted as sigmoid curve (Fig. 1Fa). The SI_{50} was defined as the stimulus intensity at which AP appeared 5 times out of 10 repeated burst inputs based on the fitting curve (Fig. 1Fa), and the values of SI_{50} for the control and pPP-LFS were normalized and compared in Fig. 1Fb. The SI_{50} significantly decreased in the neurons that underwent LTD (0.78±0.07% in the pPP-LFS, 6 neurons, *t*=3.596, p=0.016, paired *t*-test; blue, Fig. 1Fb). In Fig. 1Ga, the Max. EPSP slope is plotted on the x-axis, and the AP probability is plotted on

the y-axis and fitted as a sigmoid curve, as in Fig. 1Fa. The Max. EPSP slope (V/s) was taken from the maximal value of the first derivative of the EPSP trace (corresponding to the steepest rise in the EPSP rising phase from Fig. 1D). The ES_{50} (Fig. 1Gb) was defined as the value of the Max. EPSP slope at which the AP appeared 5 times out of 10 repeated burst inputs based on the fitting curve (Fig. 1Ga), and the values of the ES_{50} in the control and the pPP-LFS were normalized and compared. The PP-LFS induced a decrease in the value of the ES_{50} to 0.84±0.03 (6 neurons, t=4.694, p=0.005, paired t-test) compared to the control. For the SC-CA1 synapses, a previous study suggested that the E-S potentiation evoked after the PP-LFS would be correlated with the hyperpolarization of the AP threshold (V_{th}) [16]. We determined the V_{th}_TA as the membrane potential of the CA1-PCs, where dV/dt was over 10 V/s, and we found that the V_{th}_TA was significantly hyperpolarized after the PP-LFS was delivered to the TA-CA1 synapses (-39.26±1.04 to -44.38±1.08 mV; 8 neurons, t=3.678, p=0.008, paired t-test; Fig. 1Ha~Hb). The above results showed that the TA-LTD in the CA1-PCs evoked by the PP-LFS was accompanied by the PIE.

GABA blockers did not influence the intrinsic excitability changes during TA-LTD

Previously, we showed that the E-S potentiation after the PP-LFS at the SC-CA1 synapses was attributable to decreased GABAergic inputs, and the mixture of GABA receptor A ($GABA_AR$) blockers and GABA receptor B ($GABA_BR$) blockers (hereafter anti-GABARs) occluded the effects of the PP-LFS on the E-S potentiation and the V_{th} hyperpolarization without affecting the expression of the LTD [16]. To investigate whether decreased GABAergic inputs contributed to the E-S potentiation and V_{th} hyperpolarization after the PP-LFS, we performed a series of experiments, shown in Fig. 1, in the presence of anti-GABARs, the mixture of a $GABA_AR$ antagonist (bicuculline 20 μM or picrotoxin 100 μM) and a $GABA_BR$ antagonist (CGP52432 1 μM). The TA-LTD in TA-CA1 synapses was still induced by the PP-LFS despite of the presence of anti-GABARs (232.83±35.01 to 192.31±37.18 pA, 6 neurons; t=-1.094, p=0.294; paired t-test; Fig. 2Aa). The PPR of the TA-CA1 still increased after the PP-LFS despite the presence of anti-GABARs (1.36±0.05 to 1.49±0.05, 6 neurons, t=-2.639, p=0.03, paired t-test; Fig. 2Ab). These results suggest that the inhibition of GABAergic inputs would not significantly contribute to the induction of TA-LTD. The AP probability in response to the TA burst stimulation increased significantly after the PP-LFS (Fig. 2Ba) along with the V_{th} hyperpolarization in the presence of the anti-GABARs (Control, -41.67±0.89 mV; pPP-LFS, -46.92±1.41 mV; 7 neurons, t=4.083, p=0.003, paired t-test; Fig. 2Bb). The normalized SI_{50} (0.83±0.05 in the pPP-LFS, 7 neurons, t=3.303, p=0.016, paired t-test, Fig. 2Ca and 2Cb) and the normalized ES_{50} (0.91±0.03 in the pPP-LFS, 7 neurons, t=2.515, p=0.046, paired t-test; Fig. 2Da and 2Db) significantly decreased after the PP-LFS despite the anti-GABARs. These results indicate that the GABAergic mechanism was not a major contributor to the E-S potentiation of the TA-CA1 synapses induced by the PP-LFS.

As a possible mechanism underlying the increased excitability associated with synaptic LTD at the TA-CA1 synapses, we first examined the h-current (I_h) downregulation because the HCN channels, which evoke I_h, play a role in the dendritic excitability of the CA1-PCs [22], and increased excitability due to I_h downregulation during mGluR-dependent LTD has been reported [23]. However, the PP-LFS did not significantly decrease the voltage sag (a phenomenon in which the membrane potential initially shows a transient peak in response and then decays to a steady level to current injection; see Materials and Methods), which is a typical feature of I_h inhibition (PP-LFS: $F_{(1,112)}$=0.528, p=0.469, Current: $F_{(7,112)}$=23.781, p<0.001, PP-LFS×Current: $F_{(7,112)}$=0.082, p=0.999; 8 neurons; 2-way ANOVA; Supplemental Fig. 1Aa and 1Ab). These results suggest that I_h inhibition is not a major contributor to the increased excitability during TA-LTD.

The D1-dependent decrease in the K^+ current underlies the PP-LFS-induced E-S potentiation

The SLM of the CA1 receives not only the TA inputs from the entorhinal cortex but also the dopaminergic inputs from the ventral–tegmental area (VTA) or locus coeruleus (LC) and the cholinergic inputs from the nucleus basalis of Meynert (nbM) [24]. It is known that dopamine receptors, including the D1 and D2 receptors, participate in the synaptic plasticity associated with memory and behavior [25-27], and they are involved in the regulation of the voltage-dependent K^+ channels [28-30]. A previous study showed that the interaction between the dopamine receptors and mGluRs evoked afterdepolarization, which was induced by AP bursts [13]. We measured the AP latency and V_{th} evoked by the ramp current under the control or the D1/D2 receptor antagonist. The hyperpolarization of V_{th} was eliminated by application of the D1 receptor antagonist (SCH23390; Tocris, #0925, Bristol, UK) but not the D2 receptor antagonist (SCH23390; Tocris, #0925, Bristol, UK), not the D2 receptor antagonist (Sulpiride; Tocris, #0895, Bristol, UK) (Control: $F_{(1,17)}$=24.267, p<0.001, 8 neurons; SCH23390: $F_{(1,17)}$=0.432, p =0.520, 6 neurons; sulpiride: $F_{(1,17)}$=16.038, p<0.001, 6 neurons; RM-ANOVA and simple effect analysis; Fig. 3Aa and 3Ba). The number of APs evoked by the ramp current did not increase with the application of SCH23390, however, it was increased by the sulpiride (Control: $F_{(1,17)}$=10.668, p=0.005; SCH23390: $F_{(1,17)}$=0.018, p=0.894; sulpiride: $F_{(1,17)}$=4.645,

https://doi.org/10.5607/en22028

p=0.046; RM-ANOVA and simple effect analysis; Fig. 3Ab and 3Bb). The latency of the 1st AP was shortened after the PP-LFS under the control or supiride, however, application of SCH23390 abolished the shortening of AP latency after the PP-LFS (Control: $F_{(1,17)}$=13.769, p=0.002; SCH23390: $F_{(1,17)}$=0.140, p =0.713; sulpiride: $F_{(1,17)}$=5.33, p=0.034; RM-ANOVA and simple effect analysis; Fig. 3Ac and 3Bc). The parameters of intrinsic excitability were not changed despite the dopamine antagonists (V_{th}: $F_{(2,17)}$=1.026, p=0.379; AP#: $F_{(2,17)}$=0.075, p=0.928; AP latency: $F_{(2,17)}$=0.048, p=0.953; RM-ANOVA and simple effect analysis; Fig. 3A and 3B).

These results suggest that the D1 receptor-mediated downregulation of the K^+ currents mediated the downward shift of the V_{th} of the CA1-PCs after the PP-LFS. The decreased K^+ conductance (defined as membrane current/driving force) suggests that membrane resistance (R_{in}) of CA1-PCs increased after the PP-LFS. The R_{in} of CA1-PC was increased after PP-LFS in the control group and sulpride-treated group, but not in the SCH23390-treated group (Control: $F_{(1,16)}$=9.507, p=0.007, 7 neurons; SCH23390: $F_{(1,16)}$=0.783, p=0.389, 5 neurons; sulpiride: $F_{(1,16)}$=2.208, p=0.157, 5 neurons; Supplemental Fig. 3). Although the significance level for the sulpiride group was not significant, a consistent upward trend of R_{in} was observed, as shown in Supplementary Fig. 3. The K^+ conductance in the CA1-PCs decreased in both the control and sulpiride groups; the direction of change in the RMP was different in each group (Control: $F_{(1,13)}$=13.096, p=0.003; SCH23390: $F_{(1,13)}$=0.964, p=0.344; sulpiride: $F_{(1,13)}$=0.798, p=0.388; Supplemental Fig. 3). This suggests that the change in the K^+ conductance after the PP-LFS in this study did not seem to have a significant effect on the RMP.

We studied the involvement of the K^+ current inhibition evoked by dopaminergic signaling in the increased excitability by the PP-LFS. Because application of dopamine antagonist did not change parameters of intrinsic excitability *per se*, (V_{th}: $F_{(2,17)}$=3.181, p=0.067; APs: $F_{(2,17)}$=0.843, p=0.448; $F_{(2,17)}$=1.254, p=0.310; RM-ANOVA and simple main effect analysis; Fig. 3B~3D), measuring only the K^+ currents after the PP-LFS would be sufficient to explain the changes in the intrinsic excitability after the PP-LFS and the effect of the dopamine receptors on it. Since the purpose of our study was to determine which dopamine receptors were involved in the downregulation of K^+ currents induced by PP-LFS (which causes mGluR5 activation), so the effect of dopamine receptor application alone was not tested. The K^+ currents were measured by applying depolarization voltage pulses (1 s duration, 10 mV step to -30 mV~+50 mV) from the holding potential of -70 mV for the before (no PP-LFS, Fig. 3Aa) and 30 min after PP-LFS (pPP-LFS, 7 neuron, Fig. 3Ea), showing a slight decrease in the K^+ current (no PP-LFS vs. pPP-LFS: p=0.005, 2-way ANOVA and Bonferroni posthoc test; Fig. 3Eb, Table 1). Because parameters of intrinsic excitability in Fig. 3A~3D would be influenced by steady-state depolarization current (Fig. 3A, 3B), steady-state current (I_{ss}) was measured. The application of SCH23390 (6 neuron) caused a slight increase, rather than a decrease, in the K^+ current of the CA1-PCs after the PP-LFS. (no PP-LFS vs. $pPP\text{-}LFS_{SCH23390}$: p<0.001, RM-ANOVA and Bonferroni posthoc test; Fig. 3B, Table 1). However, the application of sulpiride (6 neuron) decreased the K^+ current of CA1-PC after PP-LFS, and this decrease was similar to the K^+ current of the CA1-PC measured after the PP-LFS in the control (no PP-LFS vs. $pPP\text{-}LFS_{sulpiride}$: p=0.042; pPP-LFS vs. $pPP\text{-}LFS_{sulpiride}$: p=1.00, RM-ANOVA and Bonferroni post hoc analysis; Fig. 3C, Table 1). Taken together, the downregulation of K^+ currents and the PIE after the PP-LFS that would be evoked by activation of mGluR5 and D1 receptors would be associated with lowered V_{th}, increased R_{in} after the PP-LFS.

Contribution of the dopamine receptors to the TA-LTD

We showed that dopaminergic signaling modulated the intrinsic excitability of the CA1-PCs during the PP-LFS. The interaction between the dopamine receptors and the mGluR occurred during synaptic activities, and various signal pathways that could influence synaptic modulation converged in the prefrontal pyramidal neurons [11, 13, 14, 31]. Because the modulation of the two classes of dopamine receptors was different, we studied the potential influence of two dopamine receptor antagonists (SCH23390 and sulpiride) on the synaptic plasticity of the CA1-PCs. Surprisingly, delivery of the PP-LFS under the application of either SCH23390 ($F_{(1,17)}$=4.941, 7 neurons, p=0.040; RM-ANOVA and simple main effect analysis; Fig. 4Aa) or sulpiride ($F_{(1,17)}$=6.113, 8 neurons, p=0.024; RM-ANOVA and simple main effect analysis; Fig. 4Ba) evoked the TA-LTP but not the TA-LTD, which should have occurred in the control condition. Moreover, co-blockade of D1 and D2 by the co-application of SCH23390 and sulpiride induced neither LTP nor LTD ($F_{(1,17)}$=0.009, 5 neurons, p=0.926; RM-ANOVA and simple main effect analysis; Fig. 4Ca). In contrast to the increase in PPR after the LTD induction by the PP-LFS at the TA-CA1 synapse in the control group (Fig. 1B), in the groups treated with SCH23390 or sulpiride (Fig. 4Ab and 4Bb), LTP, instead of LTD, was induced by PP-LFS and the PPR did not change (SCH23390: $F_{(1,17)}$=0.876, 6 neurons, p=0.362; sulpiride: $F_{(1,17)}$=0.079, 8 neurons, p=0.782; RM-ANOVA and simple main effect analysis; Fig. 4Ab, 4Bb). Co-application of SCH23390 and sulpiride did not change PPR after the PP-LFS ($F_{(1,17)}$=0.423, 5 neurons, p=0.524, RM-ANOVA and simple main effect analysis; Fig. 4Cc). The baseline PPR did not change despite of application of dopamine antagonists ($F_{(3,24)}$=1.517, p=0.236, 1-way ANOVA). The

Table 1. Values of K^+ current in CA1-PCs[1]

V_{mem} (mV)	no PP-LFS (pA)	pPP-LFS (pA)	+SCH23390 (pA)	+Sulpiride (pA)	Comparison between conditions (for voltage)
-30	187.3±46.1	267.9±49.3	303.9±53.3	218.0±53.3	$F_{(3,23)}$=1.076 p=0.379
-20	321.2±66.9	441.8±71.5	549.8±77.2	427.7±77.2	$F_{(3,23)}$=1.691 p=0.197
-10	571.4±89.8	717.3±95.9	932.3±103.7	733.7±103.7	$F_{(3,23)}$=2.313 p=0.103
0	1,015.9±111.2	1,077.9±118.9	1,455.0±128.5	1,124.3±128.5	$F_{(3,23)}$=2.498 p=0.085
+10	1,644.1±132.9	1,549.1±142.1	2,153.3±153.5	1,600.0±153.5	$F_{(3,23)}$=3.450 p=0.033
+20	2,358.7±169.7	2,026.0±181.4	2,921.7±195.9	2,108.3±195.9	$F_{(3,23)}$=4.407 p=0.014
+30	3,199.2±214.2	2,562.2±229.0	3,716.7±247.3	2,643.3±247.3	$F_{(3,23)}$=4.982 p=0.008
+40	3,944.9±255.1	3,116.8±272.6	4,541.6±294.4	3,203.3±294.4	$F_{(3,23)}$=5.503 p=0.005
+50	4,766.1±302.7	3,626.6±323.7	5,371.7±349.6	3,763.3±349.6	$F_{(3,23)}$=6.067 p=0.003
Comparison between V_{mem} value	Control: $F_{(8,16)}$=33.651 p<0.001	pPP-LFS: $F_{(8,16)}$=16.789 p<0.001	SCH23390: $F_{(8,16)}$=30.335 p<0.001	Sulpiride: $F_{(8,16)}$=16.528 p<0.001	

RM-ANOVA[2],
Cond (control, PP-LFS, SCH23390, Sulpride): $F_{(3,23)}$=4.413, p=0.014.
voltage (from -30 mV to +50 mV): $F_{(8,184)}$=584.902, p<0.001.
Cond×voltage: $F_{(24,184)}$=6.123, p<0.001.
[1]Caution: Because blockade of Ca^{2+} and Na^+ channels are required to measure K^+ currents, repetitive measure of K^+ current before and after the PP-LFS from same neurons is not possible.
[2]Statistical significance were stated in the text and figures using following abbreviations: n.s.: no statistical significance; *: p<.05; **: p<.01; ***: p<.005.

LTD of SC-CA1 synapses was not influenced by the co-blockade of D1 and D2 (t=2.028, 5 neurons, p=0.113; paired t-test; Fig. 4Da). Also, the PPR in the SC-CA1 increased after the PP-LFS despite the presence of the dopamine antagonists (Z=-2.023, p=0.043, Wilcoxon signed-rank test; Fig. 4Db). Considering that the LTD of the SC-CA1 synapses after the PP-LFS was accompanied with increased PPR [16], along with previous studies about the mechanisms of mGluR-LTD [32], the TA-LTD, which was induced by the PP-LFS, would be evoked by mechanisms involved with the presynaptic compartment also.

DISCUSSION

Our study showed that the TA-LTD evoked by the PP-LFS was accompanied by the PIE. The PIE was evoked by the downregulation of the K^+ currents affected by the interaction of the mGluR5 with the D1 receptor (Fig. 3). However, the synaptic regulation of the TA-CA1 synapses was determined to be rather complex. Activation of both the D1 and D2 receptors and the mGluR5 induced the LTD of the TA-CA1 synapses by the PP-LFS (Fig. 1); however, when only one of the D1 or D2 receptors and the mGluR5 were activated, the PP-LFS induced the LTP but not the LTD (Fig. 4 and 5). The results of our study revealed the effect of dopamine on the hippocampal neural circuits, thereby providing clues to the process by which dopamine contributes to synaptic plasticity, spatial learning, and memory formation in the hippocampus.

Possible mechanisms of the PIE after the PP-LFS

Previous studies showed that synaptic activity that evokes synaptic plasticity was often accompanied with PIE [22, 33]. It has been known that intrinsic excitability of neurons was regulated by various factors, including neuromodulators. Neuromodulators, such as dopamine, are also known to play an important role in the regulation of hippocampal neuron intrinsic excitability [34, 35]. Dopaminergic fibers projected to the hippocampus originate from the VTA [36] and locus ceruleus [37]. Because the D1 receptor and D2 receptor are present in the ventral CA1 area [5], we focused on the role of the D1 and D2 receptors.

https://doi.org/10.5607/en22028

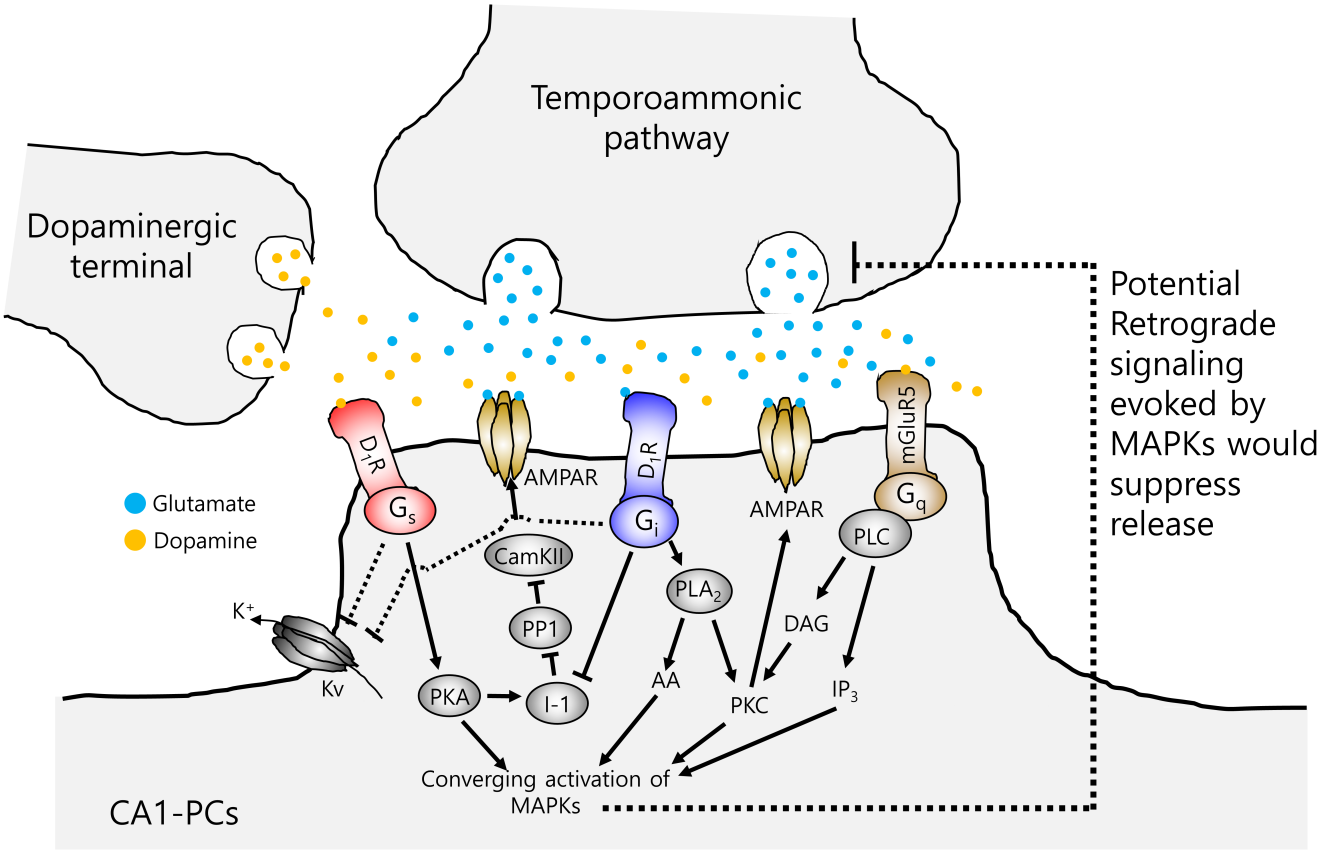

Fig. 5. Understanding input–output (I-O) plasticity during the LTD by the integration of synaptic plasticity in the TA-CA1 synapses and the E-S potentiation. Activation of the MAP kinase (MAPK) at the TA-CA1 synapse could only be activated by the simultaneous activation of the mGluR5 and two types of dopamine receptors. Activation of either the D1 receptor or D2 receptor alone may induce LTP by increasing postsynaptic AMPA conductance; however, a potential retrograde signaling, which would influence the presynaptic release, would require the converging activation of MAPKs to induce LTD. Independent from the synaptic plasticity, the activation of the D1 receptors would contribute to the PIE of the CA1-PCs by inhibiting the K^+ current.

The PP-LFS, which activates the mGluR5 and the D1 and D2 receptors in the TA-CA1 synapses, decreased the V_{th} and increased the R_{in} in the CA1-PCs (Fig. 1, Supplementary Fig. 3). These were associated with the downregulation of the K^+ conductance in the CA1-PCs and contributed to the E-S potentiation by the TA-CA1 synapses. The effect of the downregulation of the K^+ current on the RMP after the PP-LFS was slight because the direction of the RMP fluctuations in the control and sulpiride groups where the K^+ current downregulation occurred after the PP-LFS was inconsistent (Supplementary Fig. 3). In the TA-CA1 synapse, unlike the SC-CA1 synapse [16], inhibition of the GABA synapse did not affect the excitability parameters such as the E-S potentiation; so, the effect of the GABA synapse on the modulation of the TA-CA1 synapse was negligible. Taken together, the interaction between the mGluR5 and dopamine receptors induced by the PP-LFS caused the downregulation of the K^+ current. Considering the involvement of the D1 receptor and the mGluR5 in a previous study [13], the potentiation of intrinsic excitability accompanied by the TA-LTD was mediated by the D1 receptor, not the D2 receptor. However, it was reported that K^+ current modulation could occur with dopamine itself in the prefrontal cortex [38]. Considering the research results that activation of D1 and D2 receptor itself decreases or increases K^+ current [38], it is also difficult to exclude the possibility that inhibition of each receptor has already affected the baseline K^+ current. Therefore, more research on the effect of the dopamine receptor itself rather than the interaction of the mGluR5–dopamine receptor is needed.

Possible mechanisms of the TA-LTD after the PP-LFS

The most remarkable difference between the LTD of the TA-CA1 and SC-CA1 synapses was the dependency of the dopamine receptors. For the SC-CA1 synapses, blocking of the dopamine receptors did not influence the LTD induction (Fig. 4). It is known that the mGluR-LTD induction is a retrograde endocannabinoid

signal, which is evoked by protein kinase C (PKC) activated by DAG and Ca^{2+} [32], and suppresses the neurotransmitter release from the presynaptic axon terminal [32, 39]. Although a previous study showed that the action of the cannabinoid receptor type 1 in TA-CA1 synapse was insignificant [31], the potential role of cannabinoid receptors could not be ruled out due to the presence of the cannabinoid receptor type 1 in the medial perforant path synapses, which originated from the EC [40]. The TA-LTD in our study (Fig. 1) was accompanied by increased PPR, and the blockade of the mGluR5 abolished both the LTD and the change in the PPR (Supplemental Fig. 1). Considering the mechanism of the mGluR5-LTD and its signaling pathway [16, 32], the authors hypothesize that the role of mGluR5-related retrograde signals can be considered in TA-LTD.

The interaction between the mGluR5 and the dopamine receptors were studied previously in PFC pyramidal cells [14, 31, 41, 42]. Previous studies showed that activation of PKC by mGluR5 and postsynaptic D2 receptor and protein kinase A (PKA) by D1 receptor converged to activation of MAP kinase pathway, which induces downregulation of AMPA currents [11, 43]. According to aforementioned studies, D1 and D2 receptors act synergistically to produce arachidonic acid (AA) that acts as potent PKC activator in postsynaptic region [11, 44]. A previous study suggested that the synergistic activation of PKC evoked by both the mGluR5 and dopamine receptors evoked activation of MAP kinase and effectively induced LTD [11]. The PP-LFS in the control increased the PPR during the TA-LTD, which suggests the PP-LFS's effect on the TA-CA1 synapses depressed the presynaptic release (Fig. 1). Both the TA-LTD and increased PPR were abolished by the co-blockade of the D1 receptor and D2 receptor (Fig. 4C). The blockade of the D1 and D2 receptors inhibited the synergism of the dopamine receptors, thereby inhibiting the PKC, which activates MAP kinase [45], or inhibiting the production of the AA [44], a precursor of endocannabinoids [45, 46]. Based on previous studies and our data, activation of MAP kinase would cause decrease AMPA component with postsynaptic manner and retrograde signaling which would be involved with the AA and endocannabinoids. however, it is assumed that PKC activation evoked by only the mGluR5 did not induce sufficient MAP kinase activation or endocannabinoid production (Fig. 5).

Conversion to TA-LTP from TA-LTD under the dopamine antagonists

Unexpectedly, our study revealed that blockade of either the D1 or D2 receptor induced TA-LTP and not TA-LTD, after the PP-LFS. In contrast to the TA-LTD, shown in Fig. 1, there was no change in the PPR after the PP-LFS during the TA-LTP under the dopamine receptor antagonists (Fig. 4). These results suggest that the TA-LTD and TA-LTP involved mechanisms that were mainly in the presynaptic and postsynaptic regions. Previous studies suggested that activation of D1 increased PKA, which induced AMPA upregulation and subsequent postsynaptic LTP and MAP kinase activation, which downregulated the AMPA conductance and subsequently induced LTD [11, 14, 47]. Other studies in prefrontal cortex showed that the D2 receptors either activated the PKC which induced and maintained the LTP in the CA1-PCs [48] or inhibited the PKA which induced the LTP [11, 31, 43]. If either the D1 or D2 receptor were blocked, the activity of the PKC by the D2 receptor or the PKA by the D1 receptor remained and increased the AMPA component [47, 49]. However, blocking of either D1 or D2 alone is not sufficient to induce MAP kinase activity, which will result in the production of the AA, a precursor of endocannabinoids, and inhibition of AMPA components [39, 40, 45].

This study had several limitations. Although the distributions of the dopamine receptors in the hippocampus have been widely studied, the exact location of these receptors remains debated. Because the co-activation between the mGluR5 and dopamine receptors have mainly been studied in the PFC, there have been few studies on the co-activation in the hippocampus, especially the TA-CA1 synapses. Although a retrograde mechanisms affecting presynaptic release is suspected to exist, a possible candidate for the mechanisms in the TA-CA1 synapses should be studied further. Previous studies have suggested that the D1 and D2 receptors are present at the presynaptic terminal including the TA-CA1 or PFC terminals, and these receptors may function to inhibit synaptic release [50]. The potential role of presynaptic dopamine receptors needs to be further studied in the future. Given the dopamine suppression of the presynaptic domain and the signaling pathways involved in the mGluR and postsynaptic dopamine receptors, the balance between the presynaptic and postsynaptic changes induced by the PP-LFS needs to be further studied. Taking the contents of the Fig. 3 and 4 together, the TA-LTD of CA1-PCs after the PP-LFS are thought to initiate from the activation of postsynaptic mGluR5 and two types of dopamine receptors. On the other hand, PIE of CA1-PCs after PP-LFS is thought to be due to the action of the D1 receptor and mGluR5 (Fig. 5).

Physiological implication

We showed that dopaminergic projection could modulate the direct cortical inputs to the CA1-PCs. A previous study showed that TA inputs that originate from the entorhinal cortex contribute to encoding external mnemonic and sensory information [51], spatial working memory and novel recognition [4] in the hippocampus. A previous study showed that spatial representations in CA1

https://doi.org/10.5607/en22028

region was impaired by lesion of direct cortical inputs to CA1 (i.e. TA inputs) [52]. Also, dopaminergic modulation of hippocampal CA1 region was contribute to the place cell reorientation [53]. Previous study revealed that synaptic plasticity, including LTP, would be important to formation and maintenance of CA1 place field [54, 55]. However, another study revealed that the saturation of LTP prevents further learning [56]. This study suggests that stabilization and balance of the neuronal activity in a certain level would be important for the further learning and memory. This rule of balance would be applied for the LTD also. Therefore, PIE of CA1-PCs that experienced synaptic LTD would be important for maintaining the balance of neural networks in terms of homeostatic plasticity by allowing them to more sensitively receive subsequent inputs. This prediction would be consistent with previous studies [22, 57]. Taken together, dopaminergic modulation to hippocampus would contribute to maintaining hippocampal circuit stability within an appropriate level and allowing animals to smoothly recognize new information.

ACKNOWLEDGEMENTS

This research was supported by the National Research Foundation (NRF) grants from the Korean Ministry of Science and ICT (2017R1A2B2010186 to W.-K.H.).

REFERENCES

1. Bird CM, Burgess N (2008) The hippocampus and memory: insights from spatial processing. Nat Rev Neurosci 9:182-194.
2. Wixted JT, Goldinger SD, Squire LR, Kuhn JR, Papesh MH, Smith KA, Treiman DM, Steinmetz PN (2018) Coding of episodic memory in the human hippocampus. Proc Natl Acad Sci U S A 115:1093-1098.
3. Jenkins TA, Amin E, Pearce JM, Brown MW, Aggleton JP (2004) Novel spatial arrangements of familiar visual stimuli promote activity in the rat hippocampal formation but not the parahippocampal cortices: a c-fos expression study. Neuroscience 124:43-52.
4. Vago DR, Kesner RP (2008) Disruption of the direct perforant path input to the CA1 subregion of the dorsal hippocampus interferes with spatial working memory and novelty detection. Behav Brain Res 189:273-283.
5. Edelmann E, Lessmann V (2018) Dopaminergic innervation and modulation of hippocampal networks. Cell Tissue Res 373:711-727.
6. Robinson SE, Sohal VS (2017) Dopamine D2 receptors modulate pyramidal neurons in mouse medial prefrontal cortex through a stimulatory G-protein pathway. J Neurosci 37:10063-10073.
7. Yin J, Chen KM, Clark MJ, Hijazi M, Kumari P, Bai XC, Sunahara RK, Barth P, Rosenbaum DM (2020) Structure of a D2 dopamine receptor-G-protein complex in a lipid membrane. Nature 84:125-129.
8. Gurevich EV, Gainetdinov RR, Gurevich VV (2016) G protein-coupled receptor kinases as regulators of dopamine receptor functions. Pharmacol Res 111:1-16.
9. Keeler JF, Pretsell DO, Robbins TW (2014) Functional implications of dopamine D1 vs. D2 receptors: a 'prepare and select' model of the striatal direct vs. indirect pathways. Neuroscience 282:156-175.
10. Floresco SB (2013) Prefrontal dopamine and behavioral flexibility: shifting from an "inverted-U" toward a family of functions. Front Neurosci 7:62.
11. Otani S, Auclair N, Desce JM, Roisin MP, Crépel F (1999) Dopamine receptors and groups I and II mGluRs cooperate for long-term depression induction in rat prefrontal cortex through converging postsynaptic activation of MAP kinases. J Neurosci 19:9788-9802.
12. Tseng KY, O'Donnell P (2004) Dopamine-glutamate interactions controlling prefrontal cortical pyramidal cell excitability involve multiple signaling mechanisms. J Neurosci 24:5131-5139.
13. Sidiropoulou K, Lu FM, Fowler MA, Xiao R, Phillips C, Ozkan ED, Zhu MX, White FJ, Cooper DC (2009) Dopamine modulates an mGluR5-mediated depolarization underlying prefrontal persistent activity. Nat Neurosci 12:190-199.
14. Voulalas PJ, Holtzclaw L, Wolstenholme J, Russell JT, Hyman SE (2005) Metabotropic glutamate receptors and dopamine receptors cooperate to enhance extracellular signal-regulated kinase phosphorylation in striatal neurons. J Neurosci 25:3763-3773.
15. Otani S, Daniel H, Roisin MP, Crepel F (2003) Dopaminergic modulation of long-term synaptic plasticity in rat prefrontal neurons. Cereb Cortex 13:1251-1256.
16. Kim HH, Park JM, Lee SH, Ho WK (2019) Association of mGluR-dependent LTD of excitatory synapses with endocannabinoid-dependent LTD of inhibitory synapses leads to EPSP to spike potentiation in CA1 pyramidal neurons. J Neurosci 39:224-237.
17. Navakkode S, Sajikumar S, Korte M, Soong TW (2012) Dopamine induces LTP differentially in apical and basal dendrites through BDNF and voltage-dependent calcium channels. Learn Mem 19:294-299.
18. Isaac JT, Hjelmstad GO, Nicoll RA, Malenka RC (1996) Long-

term potentiation at single fiber inputs to hippocampal CA1 pyramidal cells. Proc Natl Acad Sci U S A 93:8710-8715.
19. Dvorak-Carbone H, Schuman EM (1999) Long-term depression of temporoammonic-CA1 hippocampal synaptic transmission. J Neurophysiol 81:1036-1044.
20. Kerrigan TL, Brown JT, Randall AD (2014) Characterization of altered intrinsic excitability in hippocampal CA1 pyramidal cells of the Aβ-overproducing PDAPP mouse. Neuropharmacology 79:515-524.
21. Amaral DG, Ishizuka N, Claiborne B (1990) Neurons, numbers and the hippocampal network. Prog Brain Res 83:1-11.
22. Gasselin C, Inglebert Y, Ankri N, Debanne D (2017) Plasticity of intrinsic excitability during LTD is mediated by bidirectional changes in h-channel activity. Sci Rep 7:14418.
23. Brager DH, Johnston D (2007) Plasticity of intrinsic excitability during long-term depression is mediated through mGluR-dependent changes in I(h) in hippocampal CA1 pyramidal neurons. J Neurosci 27:13926-13937.
24. Palacios-Filardo J, Mellor JR (2019) Neuromodulation of hippocampal long-term synaptic plasticity. Curr Opin Neurobiol 54:37-43.
25. Swant J, Wagner JJ (2006) Dopamine transporter blockade increases LTP in the CA1 region of the rat hippocampus via activation of the D3 dopamine receptor. Learn Mem 13:161-167.
26. Espadas I, Ortiz O, García-Sanz P, Sanz-Magro A, Alberquilla S, Solis O, Delgado-García JM, Gruart A, Moratalla R (2021) Dopamine D2R is required for hippocampal-dependent memory and plasticity at the CA3-CA1 synapse. Cereb Cortex 31:2187-2204.
27. Yang K, Broussard JI, Levine AT, Jenson D, Arenkiel BR, Dani JA (2017) Dopamine receptor activity participates in hippocampal synaptic plasticity associated with novel object recognition. Eur J Neurosci 45:138-146.
28. Neve KA, Seamans JK, Trantham-Davidson H (2004) Dopamine receptor signaling. J Recept Signal Transduct Res 24:165-205.
29. Perez MF, White FJ, Hu XT (2006) Dopamine D(2) receptor modulation of K(+) channel activity regulates excitability of nucleus accumbens neurons at different membrane potentials. J Neurophysiol 96:2217-2228.
30. Ågren R, Sahlholm K (2020) Voltage-dependent dopamine potency at D1-like dopamine receptors. Front Pharmacol 11:581151.
31. Xu TX, Sotnikova TD, Liang C, Zhang J, Jung JU, Spealman RD, Gainetdinov RR, Yao WD (2009) Hyperdopaminergic tone erodes prefrontal long-term potential via a D2 receptor-operated protein phosphatase gate. J Neurosci 29:14086-14099.
32. Bellone C, Lüscher C, Mameli M (2008) Mechanisms of synaptic depression triggered by metabotropic glutamate receptors. Cell Mol Life Sci 65:2913-2923.
33. Frick A, Johnston D (2005) Plasticity of dendritic excitability. J Neurobiol 64:100-115.
34. Fujita M, Ochiai Y, Takeda TC, Hagino Y, Kobayashi K, Ikeda K (2020) Increase in excitability of hippocampal neurons during novelty-induced hyperlocomotion in dopamine-deficient mice. Mol Brain 13:126.
35. Edelmann E, Lessmann V (2013) Dopamine regulates intrinsic excitability thereby gating successful induction of spike timing-dependent plasticity in CA1 of the hippocampus. Front Neurosci 7:25.
36. Tsetsenis T, Badyna JK, Wilson JA, Zhang X, Krizman EN, Subramaniyan M, Yang K, Thomas SA, Dani JA (2021) Midbrain dopaminergic innervation of the hippocampus is sufficient to modulate formation of aversive memories. Proc Natl Acad Sci U S A 118:e2111069118.
37. Kempadoo KA, Mosharov EV, Choi SJ, Sulzer D, Kandel ER (2016) Dopamine release from the locus coeruleus to the dorsal hippocampus promotes spatial learning and memory. Proc Natl Acad Sci U S A 113:14835-14840.
38. Yang J, Ye M, Tian C, Yang M, Wang Y, Shu Y (2013) Dopaminergic modulation of axonal potassium channels and action potential waveform in pyramidal neurons of prefrontal cortex. J Physiol 591:3233-3251.
39. Castillo PE, Younts TJ, Chávez AE, Hashimotodani Y (2012) Endocannabinoid signaling and synaptic function. Neuron 76:70-81.
40. Peñasco S, Rico-Barrio I, Puente N, Gómez-Urquijo SM, Fontaine CJ, Egaña-Huguet J, Achicallende S, Ramos A, Reguero L, Elezgarai I, Nahirney PC, Christie BR, Grandes P (2019) Endocannabinoid long-term depression revealed at medial perforant path excitatory synapses in the dentate gyrus. Neuropharmacology 153:32-40.
41. Kotecha SA, Oak JN, Jackson MF, Perez Y, Orser BA, Van Tol HH, MacDonald JF (2002) A D2 class dopamine receptor transactivates a receptor tyrosine kinase to inhibit NMDA receptor transmission. Neuron 35:1111-1122.
42. Gangarossa G, Longueville S, De Bundel D, Perroy J, HervéD, Girault JA, Valjent E (2012) Characterization of dopamine D1 and D2 receptor-expressing neurons in the mouse hippocampus. Hippocampus 22:2199-2207.
43. Guan Z, Kim JH, Lomvardas S, Holick K, Xu S, Kandel ER, Schwartz JH (2003) p38 MAP kinase mediates both short-

term and long-term synaptic depression in aplysia. J Neurosci 23:7317-7325.
44. Piomelli D, Pilon C, Giros B, Sokoloff P, Martres MP, Schwartz JC (1991) Dopamine activation of the arachidonic acid cascade as a basis for D1/D2 receptor synergism. Nature 353:164-167.
45. Maccarrone M (2017) Metabolism of the endocannabinoid anandamide: open questions after 25 years. Front Mol Neurosci 10:166.
46. Wang J, Ueda N (2009) Biology of endocannabinoid synthesis system. Prostaglandins Other Lipid Mediat 89:112-119.
47. Park P, Georgiou J, Sanderson TM, Ko KH, Kang H, Kim JI, Bradley CA, Bortolotto ZA, Zhuo M, Kaang BK, Collingridge GL (2021) PKA drives an increase in AMPA receptor unitary conductance during LTP in the hippocampus. Nat Commun 12:413.
48. Wang JH, Feng DP (1992) Postsynaptic protein kinase C essential to induction and maintenance of long-term potentiation in the hippocampal CA1 region. Proc Natl Acad Sci U S A 89:2576-2580.
49. Ren SQ, Yan JZ, Zhang XY, Bu YF, Pan WW, Yao W, Tian T, Lu W (2013) PKCλ is critical in AMPA receptor phosphorylation and synaptic incorporation during LTP. EMBO J 32:1365-1380.
50. Otmakhova NA, Otmakhov N, Lisman JE (2002) Pathway-specific properties of AMPA and NMDA-mediated transmission in CA1 hippocampal pyramidal cells. J Neurosci 22:1199-1207.
51. Ito HT, Schuman EM (2012) Functional division of hippocampal area CA1 via modulatory gating of entorhinal cortical inputs. Hippocampus 22:372-387.
52. Brun VH, Leutgeb S, Wu HQ, Schwarcz R, Witter MP, Moser EI, Moser MB (2008) Impaired spatial representation in CA1 after lesion of direct input from entorhinal cortex. Neuron 57:290-302.
53. Retailleau A, Morris G (2018) Spatial rule learning and corresponding CA1 place cell reorientation depend on local dopamine release. Curr Biol 28:836-846.e4.
54. Renaudineau S, Poucet B, Laroche S, Davis S, Save E (2009) Impaired long-term stability of CA1 place cell representation in mice lacking the transcription factor zif268/egr1. Proc Natl Acad Sci U S A 106:11771-11775.
55. Ashby DM, Floresco SB, Phillips AG, McGirr A, Seamans JK, Wang YT (2021) LTD is involved in the formation and maintenance of rat hippocampal CA1 place-cell fields. Nat Commun 12:100.
56. Moser EI, Krobert KA, Moser MB, Morris RG (1998) Impaired spatial learning after saturation of long-term potentiation. Science 281:2038-2042.
57. Zenke F, Gerstner W, Ganguli S (2017) The temporal paradox of Hebbian learning and homeostatic plasticity. Curr Opin Neurobiol 43:166-176.